Short-Through-Line Bandstop Filters Using Dual-Coupled Resonators

Andrew C. Guyette, *Senior Member, IEEE*, and Eric J. Naglich, *Member, IEEE*

***Abstract*—A new approach using dual-coupled-resonator bandstop sections to realize microwave bandstop filters with arbitrarily short through-line length is proposed. In contrast to our recent work in 2015, this approach does not require the resonator-to-through-line couplings to be comprised of both electric and magnetic coupling, i.e., mixed coupling. An exact transformation from a conventional inline bandstop filter topology to a dual-coupled-resonator bandstop filter topology is presented. A design procedure is given for both all-dual-coupled-resonator designs and mixed (single-coupled and dual-coupled-resonator) designs. A fifth-order elliptic dual-coupled-resonator microstrip prototype is presented with a center frequency of 500 MHz and a through-line length of 6.35 cm, 17% the length of a conventional design. A fifth-order elliptic mixed-resonator microstrip prototype is presented with a center frequency of 500 MHz and a through-line length of 5.01 cm, 13.7% the length of a conventional design.**

***Index Terms*—Filtering theory, microwave filters, passive filters, resonator filters.**

I. Introduction

Microwave bandstop filters are used in systems to block unwanted signals. At microwave frequencies, bandstop filters are typically implemented using resonators electromagnetically coupled to a transmission line, with spacing between couplings close to a quarter-wavelength for symmetric responses [1]–[5]. The required transmission-line lengths between resonator couplings may be fully or partially absorbed into the coupling structures used [6]. However, for technologies where strong coupling is readily available (e.g., suspended stripline), the transmission-line length associated with the coupling structures can be made quite short and, thus, extra lengths of transmission line not associated with resonator coupling must be added to realize the required phase shift between resonator sections. This extra transmission-line length adds size and insertion loss.

In [1], it was shown that extra transmission-line length can be eliminated with the use of mixed coupling (both electric and magnetic). In many resonator technologies (e.g., evanescent-mode cavity [7], ceramic coaxial, etc.) mixed coupling cannot always be practically realized. This paper addresses this issue with a more general approach, based on dual-coupled bandstop resonator sections, that does not require mixed coupling. Dual-coupled bandstop resonators were used previously in [8] for use in bandstop filters with broad upper passbands, and later in [9] for realizing self-switching tunable bandstop filters. In this paper it is shown that dual-coupled bandstop resonators are unique in that they allow for an arbitrary phase shift between adjacent cascaded sections without the need for additional lengths of transmission line. In Section II, an exact circuit transformation from a conventional single-coupled-resonator topology to a dual-coupled-resonator topology is presented. In Section III, a complete design procedure for dual-coupled-resonator bandstop filters is described, and a fifth-order elliptic dual-coupled-resonator microstrip prototype is shown with a measured center frequency of 500 MHz and a through-line length of 6.35 cm, which is 17% the length of a conventional design. Section IV presents a design procedure for mixed (single- and dual-coupled) resonator bandstop filters, which allows for even shorter through-line lengths. A fifth-order elliptic mixed-resonator microstrip prototype is presented that has a 5.01-cm through-line length, which is only 13.7% the length of a conventional design. Section V gives a comparison of the passband insertion-loss performance between dual-coupled-resonator, mixed-resonator, and conventional single-coupled-resonator bandstop filters.

II. Single-Coupled Resonator to Dual-Coupled Resonator Circuit Transformation

Shown in Fig. 1(a) is a high-pass prototype of a conventional single-coupled-resonator bandstop section. It consists of a resonator, modeled as a 1-F capacitor in parallel with a susceptance B_0, coupled to a transmission line with an admittance inverter K_0. The point at which the resonator is coupled to the transmission line is referred to here as the coupling reference plane, defined by the electrical lengths θ_1 and θ_2. Shown in Fig. 1(b) is a high-pass prototype of a dual-coupled-resonator bandstop section. It consists of a resonator, modeled as a 1-F capacitor in parallel with a susceptance B, coupled twice with admittance inverters K_1 and K_2 across a transmission line of electrical length θ_T. Following the analysis in [9], the S-parameters for the single-coupled-resonator section are

$$S_{21} = e^{-j(\theta_1+\theta_2)} \frac{p + jB_0}{p + \frac{K_0^2}{2} + jB_0} \tag{1}$$

Manuscript received May 14, 2015; revised October 21, 2015 and November 23, 2015; accepted November 28, 2015. This work was supported by the Defense Advanced Research Projects Agency (DARPA) and by the Office of Naval Research (ONR).

The authors are with Code 6851, U.S. Naval Research Laboratory (NRL), Washington, DC 20375 USA (e-mail: andrew.guyette@nrl.navy.mil; eric.naglich@nrl.navy.mil).

Color versions of one or more of the figures in this paper are available online at http://ieeexplore.ieee.org.

Digital Object Identifier 10.1109/TMTT.2015.2506631

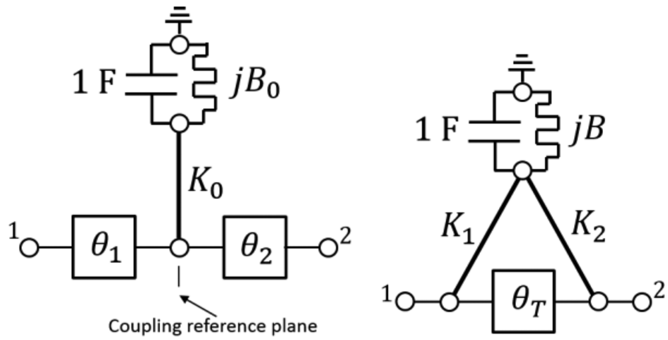

(a) (b)

Fig. 1. (a) Normalized high-pass prototype of a conventional first-order bandstop section—the coupling reference plane is defined as the point at which the inverter K_0 connects to the through line. (b) Dual-coupled bandstop section—for a given θ_T, the coupling reference plane is determined by the ratio of K_1 to K_2 and can be set to any value.

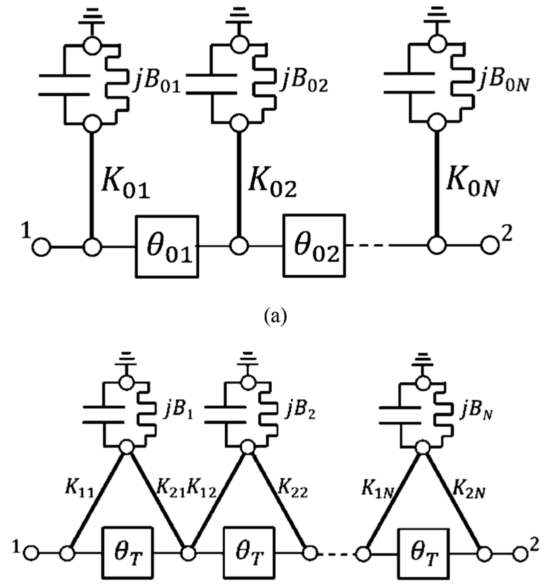

(a)

(b)

Fig. 2. (a) Conventional in-line high-pass prototype of a bandstop filter. (b) Dual-coupled-resonator high-pass prototype, where θ_T can be any value.

$$S_{11} = e^{j(\pi-2\theta_1)}\frac{K_0^2}{2p+K_0^2+j2B_0} \tag{2}$$

$$S_{22} = e^{j(\pi-2\theta_2)}\frac{K_0^2}{2p+K_0^2+j2B_0} \tag{3}$$

where p is the frequency variable $j\omega$. From (1), the single-coupled-resonator section has a transmission zero at

$$\omega = -B_0. \tag{4}$$

The S-parameters of the dual-coupled-resonator section are

$$S_{21} = \frac{j2B+2p-j2K_1K_2\sin\theta_T}{2K_1K_2+e^{j\theta_T}\left(j2B+K_1^2+K_2^2+2p\right)} \tag{5}$$

$$S_{11} = -\frac{\left(e^{j\theta_T}K_1+K_2\right)^2}{2e^{j\theta_T}K_1K_2+e^{j2\theta_T}\left(j2B+K_1^2+K_2^2+2p\right)} \tag{6}$$

$$S_{22} = -\frac{\left(K_1+e^{j\theta_T}K_2\right)^2}{2e^{j\theta_T}K_1K_2+e^{j2\theta_T}\left(j2B+K_1^2+K_2^2+2p\right)}. \tag{7}$$

The conventional and dual-coupled sections have the same transmission-zero frequency when

$$B = K_1K_2\sin\theta_T + B_0. \tag{8}$$

Replacing B from (8) into (5)–(7) gives

$$S_{21} = e^{-j\theta_T}\frac{p+jB_0}{p+jB_0+\frac{1}{2}\left(K_1^2+K_2^2+2K_1K_2\cos\theta_T\right)} \tag{9}$$

$$S_{11} = -\frac{\frac{1}{2}e^{-2j\theta_T}\left(e^{j\theta_T}K_1+K_2\right)^2}{p+jB_0+\frac{1}{2}\left(K_1^2+K_2^2+2K_1K_2\cos\theta_T\right)} \tag{10}$$

$$S_{22} = -\frac{\frac{1}{2}e^{-2j\theta_T}\left(e^{j\theta_T}K_2+K_1\right)^2}{p+jB_0+\frac{1}{2}\left(K_1^2+K_2^2+2K_1K_2\cos\theta_T\right)}. \tag{11}$$

The single-coupled-resonator and dual-coupled-resonator sections are equivalent when

$$K_0 = \sqrt{K_1^2+K_2^2+2K_1K_2\cos\theta_T} \tag{12}$$

and

$$\theta_1 = \frac{1}{2}\left(\pi + j\ln\left(-\frac{K_1/K_2+e^{-j\theta_T}}{K_1/K_2+e^{j\theta_T}}\right)\right) \tag{13}$$

$$\theta_2 = \theta_T - \theta_1. \tag{14}$$

Simultaneously solving (12) and (13) for K_1 and K_2 gives

$$K_1 = K_0\sin\theta_1(\cot\theta_T - \cot\theta_1) \tag{15}$$

$$K_2 = -K_0\csc\theta_T\sin\theta_1. \tag{16}$$

Equations (8), (15), and (16) can be used to transform a single-coupled-resonator section into an equivalent dual-coupled-resonator section. These equations are used in the dual-coupled-resonator and mixed-resonator design procedures discussed in Sections III-A and IV-A.

III. Dual-Coupled Resonator Bandstop Filters

Shown in Fig. 2(a) is a conventional high-pass prototype comprised of single-coupled-resonator sections. Shown in Fig. 2(b) is the equivalent dual-coupled-resonator prototype. A design procedure for dual-coupled-resonator filters is described in Section III-A, and a microstrip prototype designed using the procedure is presented in Section III-B.

A. Design Procedure

Step 1) Synthesize a high-pass prototype of the form shown in Fig. 3(a) that has the desired transfer function.

Step 2) Set θ_T to a desirable value. Small values of θ_T may require relatively strong coupling coefficients K_1 and K_2 from electrically short coupling structures, which may not be possible will all circuit technologies. Finding the shortest possible value of θ_T for a given response specification may require an iterative approach that is outlined in Step 3).

Step 3) Determine the input phase shift θ_{1k} for each k^{th} dual-coupled-resonator section in the dual-coupled-resonator prototype [see Fig. 2(b)] and other required parameters by performing the iterative procedure outlined in a)–h) below. The procedure is shown as a flowchart in Fig. 3.

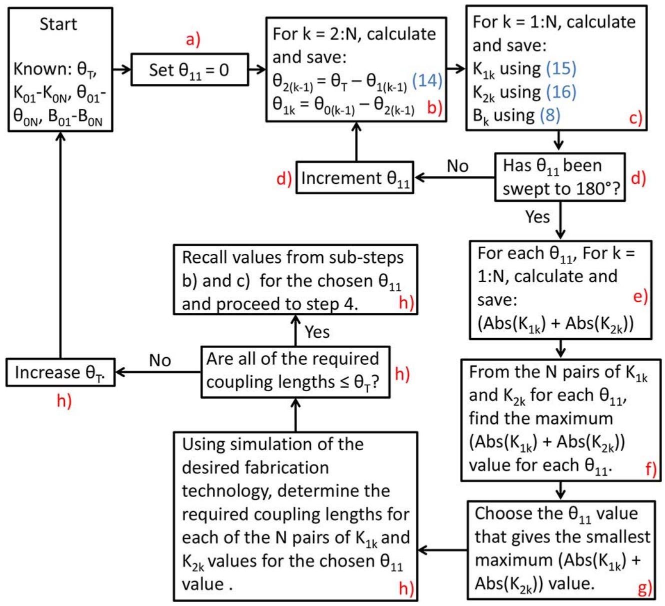

Fig. 3. Flowchart of the process in Step 3) of the filter design procedure. Blue numbers in parenthesis refer to equation numbers. Red letters with a single parenthesis refer to a)–h) of Step 3).

a) Set θ_{11}, the input phase shift of the first dual-coupled resonator section as defined in (13), equal to zero.

b) For $k = 2 - N$: calculate $\theta_{2(k-1)}$, the phase shift of the $(k-1)$th resonator, using (14). Then calculate $\theta_{1k} = \theta_{0(k-1)} - \theta_{2(k-1)}$, where $\theta_{0(k-1)}$ is the phase shift after the $(k-1)$th resonator in the high-pass prototype synthesized in Step 1) and shown in Fig. 2(a).

c) Given K_{0k}, B_{0k}, and θ_{1k} from the conventional high-pass prototype synthesized in Step 1), calculate the dual-coupled high-pass prototype values of K_{1k}, K_{2k}, and B_k for the desired θ_T using (15), (16), and (8), respectively. Save the values for each θ_{11}.

d) Check to see if θ_{11} has been incremented to 180°. If not, increment θ_{11} with an acceptable resolution increment and return to b). If yes, proceed to e).

e) For each θ_{11}, for $k = 1:N$, calculate and save the sum of the absolute values of K_{1k} and K_{2k}.

f) From the N pairs of K_{1k} and K_{2k} for each θ_{11}, find the maximum sum of the absolute values of K_{1k} and K_{2k} for each θ_{11}.

g) Choose the θ_{11} value that gives the smallest maximum sum of the absolute values of K_{1k} and K_{2k}.

h) Simulate coupling structures in the chosen resonator manufacturing technology to determine the electrical lengths required to obtain the K_{1k} and K_{2k} values for the θ_{11} chosen in g). If the sum of the required coupling lengths for each pair of K_{1k} and K_{2k} values for each resonator is shorter than θ_T, recall the values calculated in b) and c) for the chosen θ_{11} value and proceed to Step 4). If they are not shorter than θ_T, increase θ_T and restart Step 3 at a). Note that if lumped-element coupling is used for K_{1k} and K_{2k}, large coupling values can be obtained over short phase lengths, and this makes the outcome of Step 3) easier to obtain. Also note that the way Step 3) is written assumes that all θ_T values will be the same in the filter design. For the minimum total through-line length, θ_T can be different for each resonator. For this approach, f) and g) should be performed looking for the smallest average sum of the absolute values of K_{1k} and K_{2k} for all k instead of the smallest maximum sum.

Step 4) Perform a bandpass transformation to the desired center frequency and bandwidth to realize a bandstop prototype.

Step 5) Design the final filter using a desired circuit technology from the bandstop prototype. It may not be convenient to design the filter directly from the bandstop prototype, in which case each dual-coupled section can be designed using the center frequency, 3-dB bandwidth, and input phase shift θ_{1k} using the optimization or parameterization capabilities of a circuit simulator such as AWR Microwave Office. θ_{1k} can be determined from simulation using the equation

$$\theta_{1k} = -\frac{1}{2}\left(\arg\left(S_{11(k)}\right)\big|_{f=f0} + 180\right). \qquad (17)$$

B. Microstrip Prototype

As a demonstration of the proposed dual-coupled-resonator design procedure, a fifth-order elliptic-function microstrip prototype was designed, built, and tested.

Following the design procedure outlined in Section III-A, first a fifth-order elliptic high-pass prototype is synthesized using the technique described in [10]. Element values are [in reference to Fig. 2(a)] $K_{01} = 0.71315$, $K_{02} = 1.21395$, $K_{03} = 1.3377$, $K_{04} = 1.21395$, $K_{05} = 0.71315$, $B_{01} = 0.96301$, $B_{02} = 0.6426$, $B_{03} = 0$, $B_{04} = 0.6426$, $B_{05} = 0.96301$. $\theta_{01} = 72.13$,$\theta_{02} = 84.85$,$\theta_{03} = 98.16$,$\theta_{04} = 107.87$. The total through-line electrical length is 360°.

Next the conventional high-pass prototype is transformed into a dual-coupled-resonator prototype. An electrical length of 12.5° is chosen for the dual-coupled-resonator through-line electrical length θ_T, giving a total through-line length of 62.5°. Following the design procedure (Section III-A), the values of θ_{1k} are 42.50° (an arbitrarily chosen value due to the planned use of lumped-element coupling), 102.13°, 174.48°, 80.14°, and 175.51°. The resulting element values are [with reference to Fig. 2(b)] $K_{11} = 1.6475$, $K_{21} = -2.2260$, $K_{12} = 5.6086$, $K_{22} = -5.4835$, $K_{13} = 1.9119$, $K_{23} = -0.5945$, $K_{14} = 5.1870$, $K_{24} = -5.5259$, $K_{15} = 0.9628$, $K_{25} = -0.2579$, $B_1 = 0.1693$, $B_2 = -6.0140$, $B_3 = -0.2460$, $B_4 = -5.5612$, $B_5 = 0.9093$.

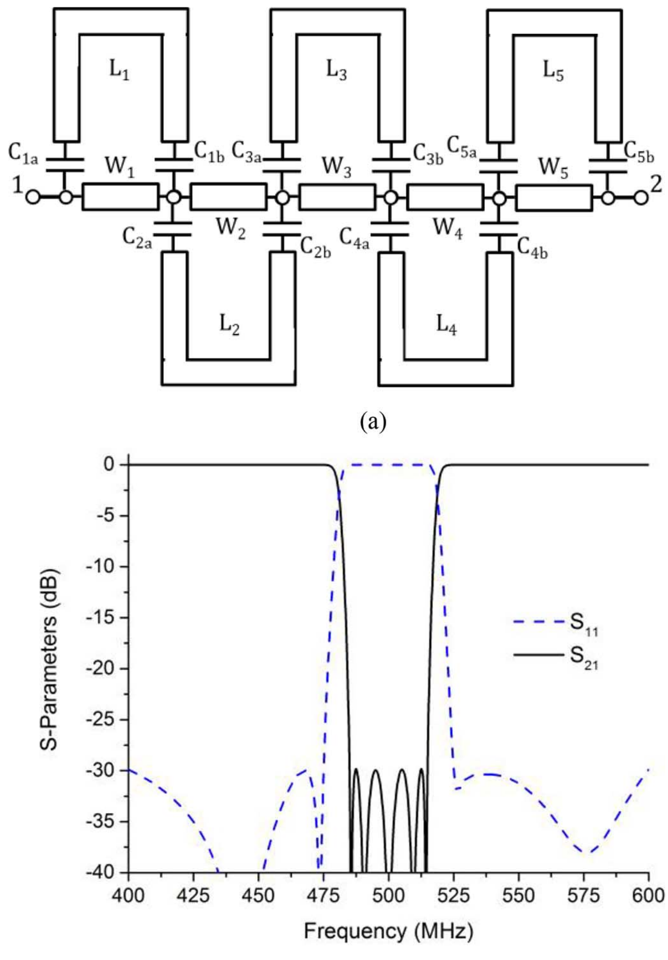

(a)

(b)

Fig. 4. (a) Schematic of the fifth-order elliptic prototype (center frequency = 500 MHz, 3-dB bandwidth = 50 MHz, 30-dB bandwidth = 30 MHz 30-dB ripple) using dual-coupled resonators. Element values are $L_1 = 138.15$ mm, $L_2 = 84.6$ mm, $L_3 = 134.98$ mm, $L_4 = 87.07$ mm, $L_5 = 122.35$ mm, $W_1 = 0.77$ mm, $W_2 = 0.28$ mm, $W_3 = 0.31$ mm, $W4 = 0.86$ mm, $W5 = 0.62$ mm, $C_{1a} = 1.29$ pF, $C_{1b} = 2.42$ pF, $C_{2a} = 4.12$ pF, $C_{2b} = 3.73$ pF, $C_{3a} = 3.37$ pF, $C_{3b} = 0.55$ pF, $C_{4a} = 2.33$ pF, $C_{4b} = 5.67$ pF, $C_{5a} = 2.43$ pF, and $C_{5b} = 1.58$ pF. All through line sections are 12.7 mm long. Substrate for the transmission lines is Rogers 4003, thickness = 1.524 mm.

The next step is to perform a standard bandpass transformation on the dual-coupled-resonator high-pass prototype, which gives a bandstop prototype, and then implement the bandstop prototype using microstrip resonators. The resonators chosen for this prototype are transmission lines capacitively coupled at opposite ends to the through-line with an electrical length of θ_T between the couplings. Coupling at opposite ends of the resonator provides the required sign difference between the two couplingsK_1 and K_2 in the dual-coupled-resonator sections for this design. At this point it is possible to synthesize the microstrip filter directly from the dual-coupled-resonator bandstop prototype, however, the authors have found that an approach using optimization in a circuit simulator to be much more time efficient and easily applicable to any type of resonator. This optimization is done on a section-by-section basis, where the primary optimization goals are transmission-zero frequency, 3-dB bandwidth, and input reflection-coefficient phase [related to θ_{1k} by (17)] at the transmission-zero frequency. These parameters are given by the bandstop prototype. A secondary optimization goal is the magnitude of the reflection coefficient in the passband frequencies, which should be small. This is important to ensure a well-matched passband. In the present case, as capacitive couplings are used, the impedance of the through line must be increased above 50 Ω to absorb the negative capacitance required to realize the admittance inverters. Shown in Fig. 4(a) is the resulting schematic-level design in AWR Microwave Office, and shown in Fig. 4(b) are simulated results using lossless components. The substrate is Rogers 4003 ($\varepsilon\ r = 3.38, \tan\delta = 0.0027$, thickness = 1.524 mm).

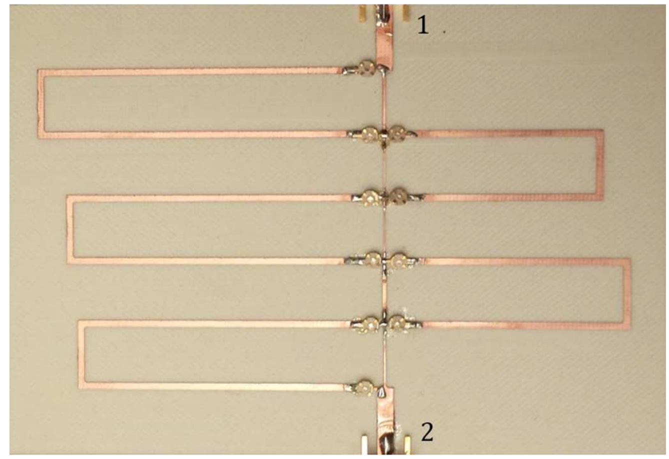

Fig. 5. Fabricated fifth-order elliptic bandstop filter prototype using dual-coupled resonators. Input is at the top of the photograph and the output is at the bottom. Dimensions correspond to the schematic design shown in Fig. 4(a). Total through-line length is 6.35 cm.

Shown in Fig. 5 is the fabricated circuit. The capacitors are Johanson 9702 trimmer capacitors. The total through-line length is 6.35 cm. Shown in Fig. 6(a) are measured narrowband results compared to an AWR Microwave Office/SONNET co-simulation. The center frequency is 500 MHz, the 3-dB bandwidth is 42.5 MHz, the 30-dB bandwidth is 23.6 MHz, and the passband insertion loss is 0.22 dB (including connector losses) at 600 MHz. Shown in Fig. 6(b) are the measured broadband results. The upper passband begins to degrade above 800 MHz due to strong coupling to the second-order modes of the resonators.

IV. Mixed-Resonator Bandstop Filters

When the input phase shift θ_{1k} for a given dual-coupled resonator section falls within the electrical length of the through-line phase length θ_T, i.e., $0 < \theta_{1k} < \theta_T$, the dual-coupled-resonator section can be realized with two couplings of the same sign, or preferably with a conventional bandstop resonator section [see Fig. 1(a)] with $\theta_1 = \theta_{1k}$ and $\theta_2 = 0$. This further decreases the total through-line length. Section IV-A outlines a design procedure.

A. Design Procedure

Step 1) Synthesize a high-pass prototype of the form shown in Fig. 2(a) giving the desired transfer function.

This article has been accepted for inclusion in a future issue of this journal. Content is final as presented, with the exception of pagination.

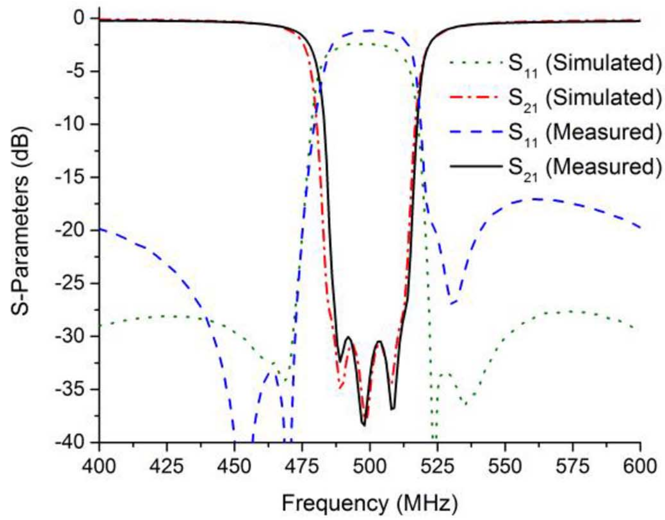

(a)

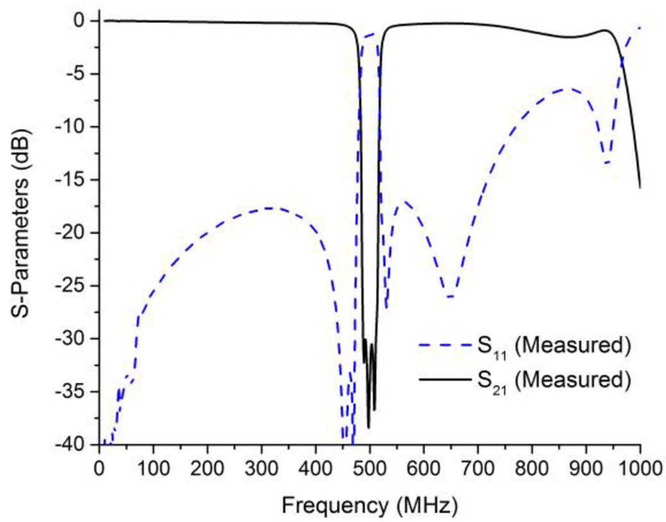

(b)

Fig. 6. (a) Measured S-parameters of the short-through-line microstrip prototype shown in Fig. 5 versus simulation (SONNET/AWR Microwave Office). (b) Broadband measured S-parameters of the short-through-line prototype.

Step 2) Calculate the input phase shift θ_{1k} for each first-order section by following a)–e) below. This is an iterative procedure that maximizes the number of conventional bandstop sections.

a) Choose a convenient value of θ_T.

b) Assign a value to θ_{11}.

c) For $k = 2 - N$: $\theta_{1k} = \theta_{0k-1} - \theta_{2k-1}$. For every section, if $0 < \theta_{1k} < \theta_T$, a conventional bandstop section is used [see Fig. 1(a)] with $\theta_1 = \theta_{1k}$ and $\theta_2 = 0$.

d) Assess and record the total through-line length.

e) Return to b) and choose a different θ_{11}. Repeat until θ_{11} has been swept from 0° to 180° with acceptable resolution. Choose the value of θ_{11} that results in the minimum total through-line length.

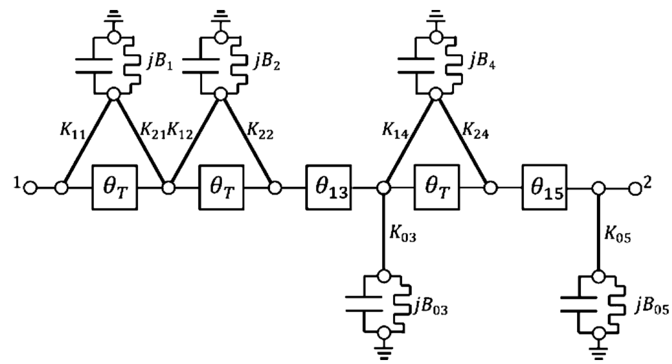

Fig. 7. Implementation of the fifth-order elliptic bandstop filter using first-order dual-coupled-resonator bandstop sections with 14.32° through-lines and single-coupled-resonator sections (total through-line length is 57.3°). Following the design procedure (Section IV-A), the values of θ_{1k} are 57.29°, −64.90°, 2.63°, −81.84°, and 11.70°. The resulting element values are $K_{11} = 1.9646, K_{21} = -2.4254, K_{12} = -4.8203, K_{22} = 4.4435, K_{13} = -1.0969, K_{23} = -0.2471, K_{14} = -4.8783, K_{24} = 4.8571, K_{15} = -0.1321, K_{25} = -0.5845$, $B_1 = -0.215887, B_2 = -4.6564, B_3 = 0.0671, B_4 = -6.5048, B_5 = -0.9439$. For the single-coupled-resonator bandstop sections $K_{03} = 1.3377, K_{05} = 0.71315, B_{03} = 0$, and $B_{05} = 0.96301$.

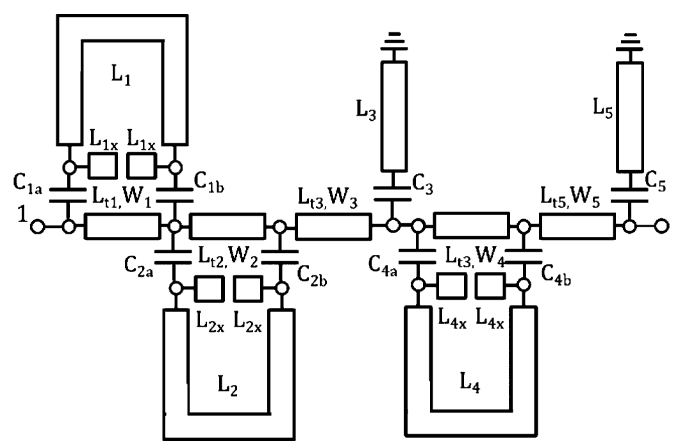

Fig. 8. Schematic of the fifth-order elliptic prototype (center frequency = 500 MHz, 3-dB bandwidth = 50 MHz, 30-dB bandwidth = 30 MHz 30-dB ripple) using dual-coupled resonators and single-coupled resonators. Element values are $L_1 = 79.07$ mm, $L_2 = 77.62$ mm, $L_3 = 71.09$ mm, $L_4 = 79.90$ mm, $L_5 = 79.30$ mm, $L_{1x} = 36.07$ mm, $L_{2x} = 22.79$ mm, $L_{4x} = 5.59$ mm, $W_1 = 0.59$ mm, $W_2 = 0.27$ mm, $W_3 = 0.63$ mm, $W_4 = 0.30$ mm, $W_5 = 0.30$ mm, $C_{1a} = 2.01$ pF, $C_{1b} = 3.01$ pF, $C_{2a} = 4.25$ pF, $C_{2b} = 2.4$ pF, $C_3 = 1.56$ pF, $C_{4a} = 3.55$ pF, $C_{4b} = 3.51$ pF, $C_{5a} = 0.83$ pF. $L_{t1} = L_{t2} = L_{t4} = 14.58$ mm, $L_{t3} = 3.92$ mm, and $L_{t5} = 1.66$ mm. Substrate for the transmission lines is Rogers 4003, thickness = 1.524 mm, $\varepsilon_r = 3.38$, $\tan\delta = 0.0027$.

Step 3) Given K_{0k}, B_{0k}, and θ_{1k}, calculate the dual-coupled low-pass prototype values of K_{1k}, K_{2k}, and B_k for a desired θ_T. For the conventional bandstop sections, $K_0 = K_{0k}$, $\theta_1 = \theta_{1k}$, and $\theta_2 = 0$.

Step 4) Perform a bandpass transformation to the desired center frequency and bandwidth.

Step 5) Realize final filter from bandstop prototype (see Step 5) in Section III-A).

This article has been accepted for inclusion in a future issue of this journal. Content is final as presented, with the exception of pagination.

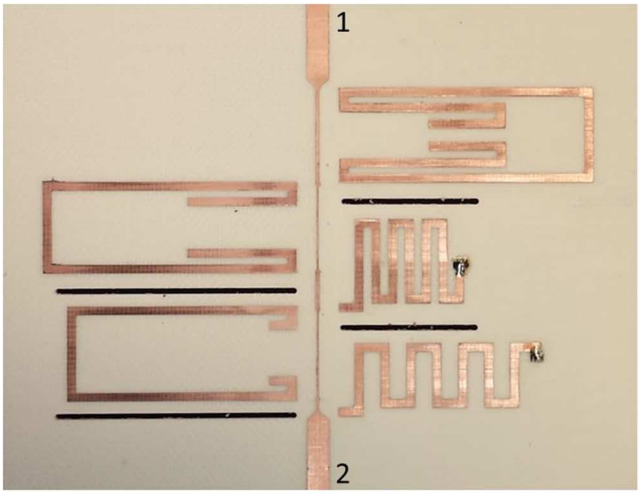

(a)

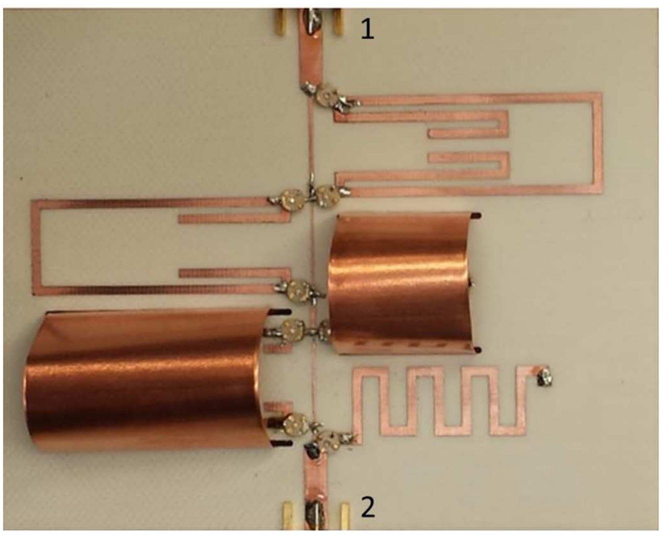

(b)

Fig. 9. Fabricated fifth-order elliptic bandstop filter prototype using both dual-coupled and conventional resonators. (a) Unpopulated circuit and (b) populated circuit. Input is at the top of the photograph and the output is at the bottom. Dimensions correspond to the schematic design shown in Fig. 8. Total through-line length (not counting 50-Ω sections at input and output) is 5.01 cm.

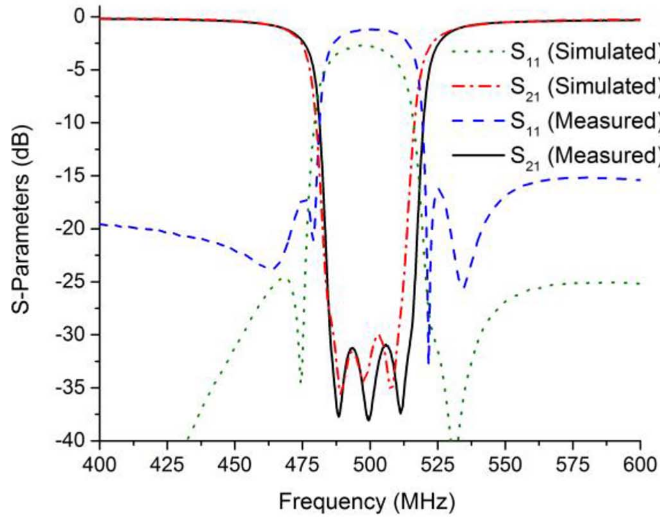

(a)

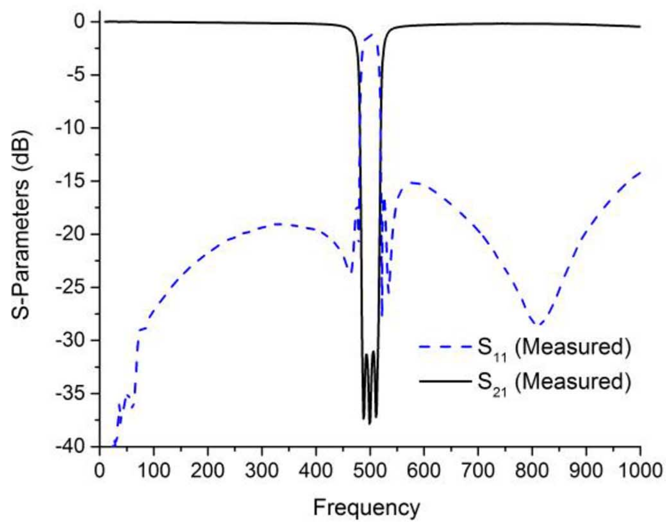

(b)

Fig. 10. (a) Measured S-parameters of the short-through-line microstrip prototype shown in Fig. 9 versus simulation (SONNET/AWR Microwave Office). (b) Broadband measured S-parameters of the short-through-line prototype.

B. Microstrip Prototype

Shown in Fig. 7 is a fifth-order mixed-resonator high-pass prototype synthesized using the approach presented in Section IV-A. The total through-line length is 57.3°.

Shown in Fig. 8 is the schematic-level design in AWR Microwave Office. This circuit was designed using the section-by-section optimization approach described in Section III-B. The resonators for this prototype have been modified from the prototype presented in Section III-B in that the location of the couplings have been offset from the ends of the resonators in order to suppress coupling to the second-order harmonic resonance and improve the upper passband. Due to the very short through-line lengths the resonators are spaced very close together and, thus, RF shields are added in the fabricated design in order to prevent distortion of the response caused by unwanted inter-resonator coupling.

Shown in Fig. 9(a) is the fabricated filter before the Johanson 9702 trimmer capacitors, connectors, and RF shields are attached. Slots are routed through the substrate to accommodate the RF shields. Shown in Fig. 9(b) is the complete filter populated with components. The RF shields are 10-mil-thick copper sheets cut to size. The total through-line length is 5.01 cm.

Shown in Fig. 10(a) are measured narrowband results compared to AWR Microwave Office/SONNET co-simulation. The measured center frequency is 500 MHz, the 3-dB bandwidth is 47.8 MHz, the 30-dB bandwidth is 29.8 MHz, and the passband insertion loss is 0.19 dB (including connector losses) at 600 MHz. Shown in Fig. 10(b) are the measured broadband results. The upper passband extends to over 1 GHz, a significant improvement over the all-dual-coupled-resonator design presented in Section III-A. Another advantage over the all-dual-coupled-resonator design is ease of post-fabrication tuning due to the fixed coupling-reference-plane offsets of the single-coupled resonators.

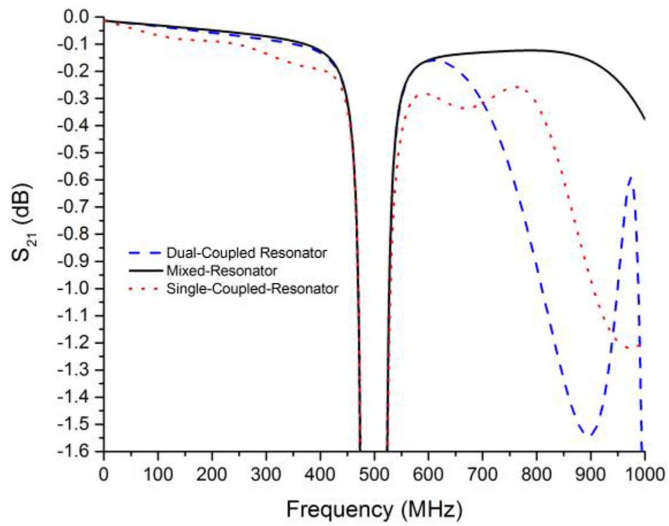

Fig. 11. Simulated insertion loss for fifth-order elliptic-function dual-coupled-resonator, mixed-resonator, and single-coupled-resonator filters. All simulations circuits are comprised of the same components as the prototypes presented in Sections III and IV.

V. Passband Insertion-Loss Comparison

The use of dual-coupled resonators allows for a significant decrease in the total through-line length of a bandstop filter compared to a conventional single-coupled-resonator topology, however, this does not necessarily come with a corresponding one-to-one decrease in passband insertion loss. In the case of very narrow bandstop bandwidths, the reactive loading effects of the couplings on the through-line can be neglected and, thus, the impedance of the through-line can remain approximately 50 Ω. Larger bandstop bandwidths require stronger resonator-through-line couplings that reactively load the through line, and in order to maintain good passband return loss the characteristic impedance of the through-line is increased to compensate, which, in turn, can increase insertion loss. This loading effect occurs in both dual- and single-coupled resonator bandstop filters, but due to the differing coupling strength and number of couplings between the two topologies, the relationship between passband insertion loss improvement and decreased through-line length is not a simple one.

Shown in Fig. 11(a) are simulations of the fifth-order dual-coupled-resonator prototype (Section III-B), the fifth-order mixed-resonator prototype (Section IV-B), and a conventional fifth-order single-coupled resonator filter (using the same components as the other two). The roll-off in passband insertion loss in the dual-coupled-resonator filter is due to poor passband match resulting from the first spurious mode of the resonators. All filters are well matched (>20-dB return loss) in the passbands. Comparing the upper passband insertion loss at 650 MHz, the single-coupled-resonator filter gives 0.33 dB, the dual-coupled-resonator filter gives 0.192 dB, and the mixed-resonator filter gives 0.138 dB. The mixed-resonator-filter has 41% of the passband insertion loss of the single-coupled-resonator filter. While a significant improvement, this is larger than the 13.7% relative length of the through line. This can be explained by the larger overall reactive loading experienced by the through-line in the mixed-resonator filter due to the larger number of couplings, requiring the average through-line impedance to be higher than that of a single-coupled-resonator filter. The through-line impedance of the single-coupled-resonator filter is 57.6 Ω (2.8 mm wide), while the average through-line impedance of the mixed-coupled-resonator filter is 139 Ω (0.34 mm wide). It is important to note that passband insertion-loss improvement is technology specific. For example, a technology with higher impedance resonators will exhibit less of a coupling-loading effect for a given 3-dB stopband bandwidth (i.e., weaker coupling required for a given coupling coefficient), and therefore a greater passband insertion loss improvement when dual-coupled resonators are used.

VI. Conclusion

This paper has presented a new general design approach for microwave bandstop filters, which allows for a considerable decrease in total through-line length compared to conventional designs. The minimum through-line length is determined only by practical considerations. Two design procedures have been presented, one for all-dual-coupled resonators and the other for mixed resonators, along with two fifth-order prototypes, which support the design procedures. The mixed-resonator prototype has a total through-line length of only 5.01 cm, 13.7% the length of a conventional design. It is expected that this work will find application whenever size and passband insertion loss is a consideration in bandstop filter design.

Acknowledgment

The views, opinions, and/or findings contained in this paper are those of the authors and should not be interpreted as representing the official views or policies of the Department of Defense or the U.S. Government.

References

[1] E. J. Naglich and A. C. Guyette, "Microwave bandstop filters with minimum through-line length," in *IEEE MTT-S Int. Microw. Symp. Dig.*, Phoenix, AZ, USA, May 17–22, 2015.

[2] L. Young, G. Matthaei, and E. Jones, "Microwave bandstop filters with narrow stop bands," in *PGMTT Nat. Symp. Dig.*, May 1962, vol. 62, no. 1, pp. 46–51.

[3] W.-H. Tu and K. Chang, "Compact second harmonic-suppressed bandstop and bandpass filters using open stubs," *IEEE Trans. Microw. Theory Techn.*, vol. 54, no. 6, pp. 2497–2502, Jun. 2006.

[4] J.-Y. Shao and Y.-S. Lin, "Millimeter-wave bandstop filter with absorptive stopband," in *IEEE MTT-S Int. Microw. Symp. Dig.*, Jun. 2014, pp. 1–4.

[5] R. Levy, R. V. Snyder, and S. Shin, "Bandstop filters with extended upper passbands," *IEEE Trans. Microw. Theory Techn.*, vol. 54, no. 6, pp. 2503–2515, Jun. 2006.

[6] H. Bell, "L-resonator bandstop filters," *IEEE Trans. Microw. Theory Techn.*, vol. 44, no. 12, pp. 2669–2672, Dec. 1996.

[7] J. Lee, E. J. Naglich, H. H. Sigmarsson, D. Peroulis, and W. J. Chappell, "Tunable inter-resonator coupling structure with positive and negative values and its application to the field-programmable filter array (FPFA)," *IEEE Trans. Microw. Theory Techn.*, vol. 59, no. 12, pp. 3389–3400, Dec. 2011.

[8] A. C. Guyette, "Design of fixed- and varactor-tuned bandstop filters with spurious suppression," in *40th Eur. Microw. Conf.*, Paris, France, Sep. 28–Sep. 30, 2010, pp. 288–291.

[9] A. C. Guyette, "Intrinsically switched varactor-tuned filters and filter banks," *IEEE Trans. Microw. Theory Techn.*, vol. 60, no. 4, pp. 1044–1056, Apr. 2012.

[10] J. D. Rhodes, "Waveguide bandstop elliptic function filters," *IEEE Trans. Microw. Theory Techn.*, vol. MTT-20, no. 11, pp. 715–718, Nov. 1972.

Andrew C. Guyette (M'08–SM'15) was born in Grand Forks, ND, USA, in 1976. He received the B.S. and M.S. degrees in electrical engineering from the University of Hawaii at Manoa, Honolulu, HI, USA, in 1999 and 2001, respectively, and the Ph.D. degree from The University of Leeds, Leeds, U.K., in 2006.

Since 2007 he has been with the Naval Research Laboratory, Washington, DC, USA. His research interests include tunable filters, lossy filters, and network synthesis.

Eric J. Naglich (S'09–M'14) received the B.S. and Ph.D. degrees in electrical and computer engineering from Purdue University, West Lafayette, IN, USA, in 2007 and 2013, respectively.

From 2007 to 2009, he was with GE Healthcare, where he was involved with the Edison Engineering Development Program. In February of 2014, he joined the U.S. Naval Research Laboratory (NRL), Washington, DC, USA, where his current research is focused on reconfigurable filter and passive circuit synthesis and fabrication techniques.

Dr. Naglich is a 2013 Karle Fellow and was a National Defense Science and Engineering Graduate (NDSEG) Fellow.